PHYSICAL REVIEW D **94,** 104006 (2016)

Charged Proca stars

Ignacio Salazar Landea[1,*] and Federico García[2,†]

[1]*Centro Atómico Bariloche, 8400 San Carlos de Bariloche, Río Negro, Argentina*
[2]*Instituto Argentino de Radioastronomía (CCT La Plata, CONICET), C.C. 5, 1894 Villa Elisa, Argentina and Facultad de Ciencias Astronómicas y Geofísicas, Universidad Nacional de La Plata, Paseo del Bosque, B1900FWA La Plata, Argentina*

(Received 14 August 2016; published 3 November 2016)

In this paper, we study gauged solutions associated with a massive vector field representing a spin-1 condensate, namely, the Proca field. We focus on regular spherically symmetric solutions which we construct either using a self-interaction potential or general relativity in order to glue the solutions together. We start generating nongravitating solutions—so-called Proca Q-balls and charged Proca Q-balls. Then we turn on backreaction on the metric, allowing gravity to hold together the Proca condensate, to study the so-called Proca stars, charged Proca stars, Proca Q-stars, and charged Proca Q-stars.

DOI: 10.1103/PhysRevD.94.104006

I. INTRODUCTION

Boson stars are gravitationally bounded macroscopic states made up of bosons. First introduced in [1,2] as spherically symmetric solutions of the Einstein-Klein-Gordon equations, they continue to be objects of study [3,4]. Of particular interest are their possible astrophysical applications, running from black-hole mimickers [5–8] and black-hole hair and clouds [9–15] to dark matter candidates [16]. Being simple tractable objects, they serve also as toy models helpful for understanding the interplay between field theory and general relativity and its possible extensions [17].

In order to construct boson stars, a fundamental aspect to be considered is the existence of an internal $U(1)$ symmetry, which will introduce an associated conserved charge that may give rise to classical solutions with nonzero total charge. Thus, a natural step forward is to gauge the global $U(1)$ symmetry. This was first done in [18], giving birth to the so-called charged boson stars.

An important family of classical objects was introduced in [19], where regular solutions for the nongravitating Klein-Gordon equation of motion were found, known as Q-balls. These objects also rely on the existence of a conserved charge and can be obtained through the minimization of their corresponding free energy. Since gravity does not glue these solutions together, the parameters of their self-interaction potentials must have the right values in order to achieve actual solutions. Some interesting general properties were presented in [20–22]. Gauged extensions to these particular classes were presented in [23].

When coupled to gravity, Q-balls become Q-stars [24,25]. Several other potentials that would not give regular spherical solutions if not coupled to gravity but that are of theoretical importance in other field theoretical contexts were also studied under this framework [26–30].

Recently, new models of boson stars and Q-balls where presented in [31,32]. In these works, a vector field representing a spin-1 condensate is studied, namely, the Proca field. Hence, those particular solutions are the Proca stars and Proca balls, respectively. In this paper, we study gauged extensions to these models, the so-called charged Proca balls and stars. For completeness, we also consider self-interacting gauged and nongauged gravitating solutions, which we shall call Proca Q-stars.

Real vector solutions were also studied in the literature [33,34] in the context of dark matter cores and accretion in compact objects. Without an internal symmetry, these solutions cannot be static and correspond to the vector equivalent of the scalar oscillatons introduced in [35].

The paper is organized as follows: in Sec. II, we present our general model; in Sec. III, we study nongravitating solutions, i.e., Proca Q-balls and charged Proca Q-balls; and, in Sec. IV, we turn on backreaction in the metric, allowing gravity to glue together the Proca condensate, giving rise to solutions named Proca stars, charged Proca stars, Proca Q-stars, and charged Proca Q-stars. Finally, in Sec. V, we summarize our results and propose some possible future directions.

II. THE MODEL

By means of introducting a vector field representing a spin-1 condensate—namely, the Proca field—we arrive at the Maxwell-Einstein-Proca model, whose action reads

$$S = \int d^4x\sqrt{-g}\left(R - \frac{1}{2}\bar{B}^{\mu\nu}B_{\mu\nu} - U(\bar{B}^{\mu}B_{\mu}) - \frac{1}{4}F^{\mu\nu}F_{\mu\nu}\right), \tag{1}$$

*peznacho@gmail.com
†fgarcia@iar-conicet.gov.ar

where $F_{\mu\nu} = \nabla_\mu A_\nu - \nabla_\nu A_\mu$ is the $U(1)$ gauge-field strength and $B_{\mu\nu} = D_\mu B_\nu - D_\nu B_\mu$, with $D_\mu = \nabla_\mu - iqA_\mu$. A similar Lagrangian with a negative cosmological constant was recently studied in [36,37] in the context of AdS/CFT duality as a model for holographic p-wave superfluids.[1]

Varying the action introduced above (1), we derive the following equations of motion:

$$D^\nu B_{\nu\mu} - U'(\bar{B}^\mu B_\mu) = 0, \tag{2}$$

$$\nabla^\nu F_{\nu\mu} - iq(B^\nu \bar{B}_{\nu\mu} - \bar{B}^\nu B_{\nu\mu}) = 0, \tag{3}$$

$$R_{\mu\nu} - \frac{1}{2} R g_{\mu\nu} = T^{(B)}_{\mu\nu} + T^{(F)}_{\mu\nu}, \tag{4}$$

where $R_{\mu\nu}$ is the Ricci tensor and $T_{\mu\nu}$ the energy-momentum tensor of the matter fields.

The energy-momentum tensor has two different components. The first one, associated with the Proca field, reads

$$T^{(B)}_{\mu\nu} = -B_{\mu\lambda}\bar{B}^\lambda_\nu - \bar{B}_{\mu\lambda}B^\lambda_\nu + \frac{1}{2} g_{\mu\nu} B_{\sigma\lambda}\bar{B}^{\sigma\lambda} - U'(\bar{B}^\mu B_\mu)(B_\mu \bar{B}_\nu + \bar{B}_\mu B_\nu) + U(\bar{B}^\mu B_\mu) g_{\mu\nu}, \tag{5}$$

while the second one, associated with the Maxwell field, is

$$T^{(F)}_{\mu\nu} = -F_{\mu\lambda}F^\lambda_\nu + \frac{1}{2} g_{\mu\nu} F_{\sigma\lambda}F^{\sigma\lambda}. \tag{6}$$

Since the model is invariant under $U(1)$, a Noether current associated with this symmetry arises. This current is defined by

$$j^\mu = \frac{1}{2}(\bar{B}^{\mu\nu} B_\nu - B^{\mu\nu}\bar{B}_\nu). \tag{7}$$

III. CHARGED PROCA BALLS

In this section we study nongravitationally bounded solutions commonly called "balls" [19] in the literature. For this purpose, we consider a fixed Minkowski metric associated with a background flat space given by

$$ds^2 = -dt^2 + dr^2 + r^2 d\Omega_2^2. \tag{8}$$

In order to achieve actual solutions for these nontopological solitons, a self-interacting potential U is needed, which we define

$$U(\bar{B}^\mu B_\mu) = m^2 \bar{B}^\mu B_\mu + \frac{\lambda}{2}(\bar{B}^\mu B_\mu)^2 + \frac{h}{3}(\bar{B}^\mu B_\mu)^3. \tag{9}$$

Here, m is the mass of the boson, while λ and h are coupling constants. The simplest spherically symmetric ansatz that admits nontrivial radial profiles reads

$$B = e^{i\omega t}(u(r)dt + iv(r)dr); \qquad A = A_t(r)dt. \tag{10}$$

In this case, the equations of motion reduce to

$$\begin{aligned} u'' - (\omega + qA_t)\left(\frac{2}{r}v + v'\right) + \frac{2}{r}u' - hu^5 + (g + 2hv^2)u^3 - (m^2 + gv^2 + hv^4)u - qvA_t = 0, \\ (-m^2 + \omega^2 + qA_t(2\omega + qA_t))v + ((u^2 - v^2)(g - h(u^2 - v^2)))v - (\omega + qA_t)u' = 0, \\ A_t'' + \frac{2}{r}A_t' + 2qvu' - 2q(\omega + qA_t)v^2 = 0. \end{aligned} \tag{11}$$

Under these assumptions, it follows that, near the origin, the fields must behave as

$$\begin{aligned} u(r) &\approx u_{(0)} - \frac{1}{6}((qA_{t(0)} + \omega)^2 + gu_{(0)}^2 - hu_{(0)}^4 - m^2)u_{(0)}r^2 + O(r^4), \\ v(r) &\approx -\frac{1}{3}(qA_{t(0)} + \omega)u_{(0)}r + O(r^3), \\ A_t(r) &\approx A_{t(0)} - \frac{1}{90}q(gA_{t(0)}^2 - hA_{t(0)}^4 - m^2)A_{t(0)}^2(qA_{t(0)} + \omega)r^4 + O(r^6). \end{aligned} \tag{12}$$

Then, in order to shoot to the desired asymptotic behavior at a fixed ω, we can use the free parameters $u_{(0)}$, $A_{t(0)}$ at the origin, naturally setting the constraint $\omega^2 < m^2$, as the asymptotic behavior reads

[1] A nonminimal coupling term $iq\gamma B_\mu \bar{B}_\nu F^{\mu\nu}$ characterizing the magnetic moment of the vector field could be an interesting extension to this model (see, for instance, [14,37]).

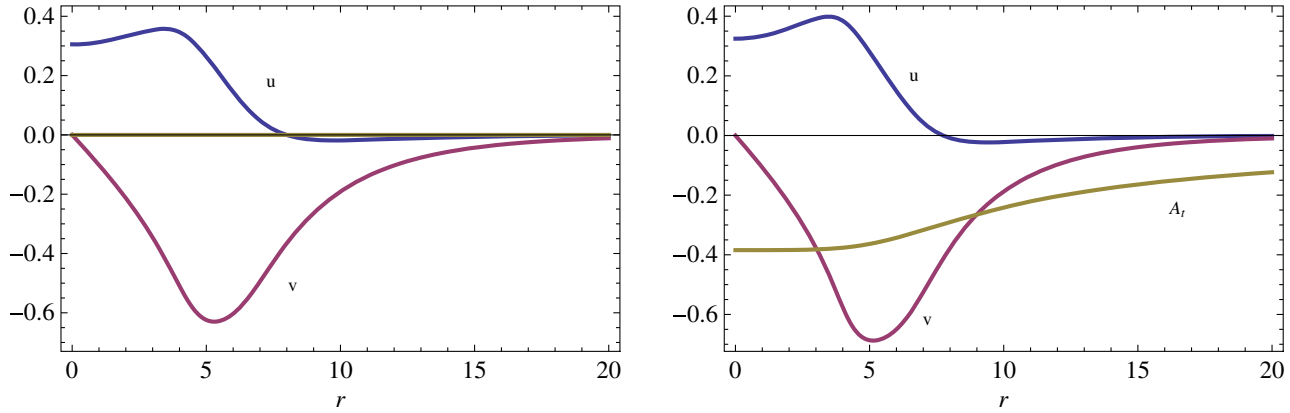

FIG. 1. Profiles for the uncharged (left panel) and charged (right panel, $q = 0.02$) solutions for $\omega = 0.980$.

$$u(r) \to c_\infty e^{-\sqrt{m^2-\omega^2}},$$
$$v(r) \to \frac{c_\infty \omega}{-\sqrt{m^2-\omega^2}} e^{-\sqrt{m^2-\omega^2}},$$
$$A_t(r) \to \frac{A_\infty}{r}. \tag{13}$$

To ensure that the trivial solution is an absolute minimum of the energy $E = \int d^3x\sqrt{-g}\epsilon = \int d^3x\sqrt{-g}T^0_0$, the potential parameters must satisfy the relation

$$h > \frac{\lambda^2}{4m^2}. \tag{14}$$

We are interested in solutions with a fixed value of the Noether charge $Q = \int d^3x\sqrt{-g}\,\rho = \int d^3x\sqrt{-g}j^0$, where the nontopological solitons are the extrema of the $F = E - \omega Q$ functional.

A. Results

Considering $m^2 = -\lambda = h = 1$ for the numerics, we found solutions with charges up to $q_{\max} = 0.03$. On Fig. 1 we show the field profiles obtained for two such typical cases: $q = 0$ and $q = 0.02$.

Writing explicity the charge and the energy density, we obtain

$$\epsilon = u'^2 + \omega^2 v^2 - 2\omega v u' + m^2(u^2+v^2) + \frac{\lambda}{2}(-3u^4 + 2u^2v^2 + v^4) + \frac{h}{3}(u^2-v^2)^2(5u^2+v^2) + \frac{1}{2}A_t'^2, \tag{15}$$

$$\rho = 2(\omega + qA_t)v^2 - vu'. \tag{16}$$

In Fig. 2, we plot ρ and ϵ profiles for the same cases described above.

On the other hand, the dependences of E and Q are presented in Fig. 3 as functions of the soliton frequency. In this figure we present the entire range for ω that we managed to reach by means of our numerical code. There are two particular limits at which the energy and the Noether charge tend to infinity. These limits correspond to the so-called thin-wall regime (when $\omega \to \omega_{\min}$) and the

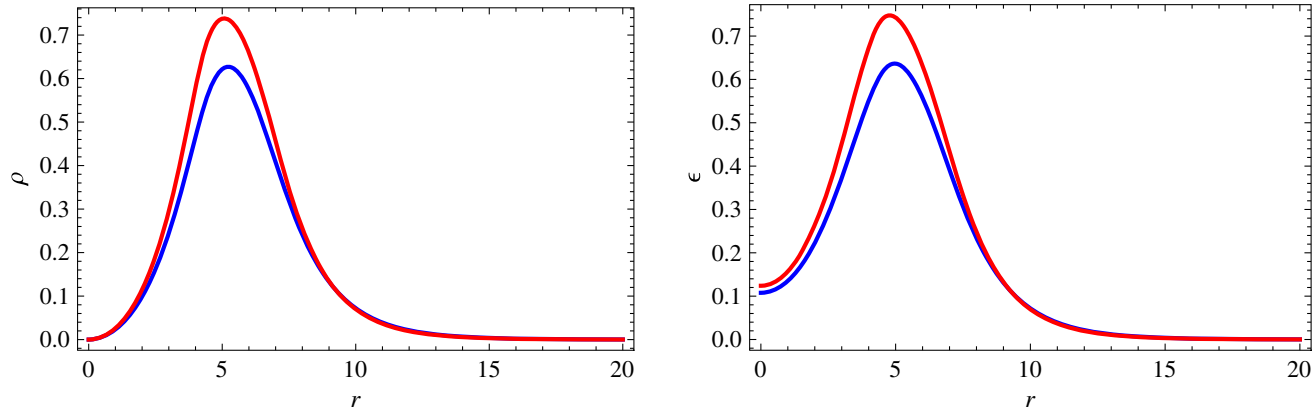

FIG. 2. Charge (left panel) and energy (right panel) density profile for the charged ($q = 0.02$, red curves) and uncharged (blue curves) solutions for $\omega = 0.980$.

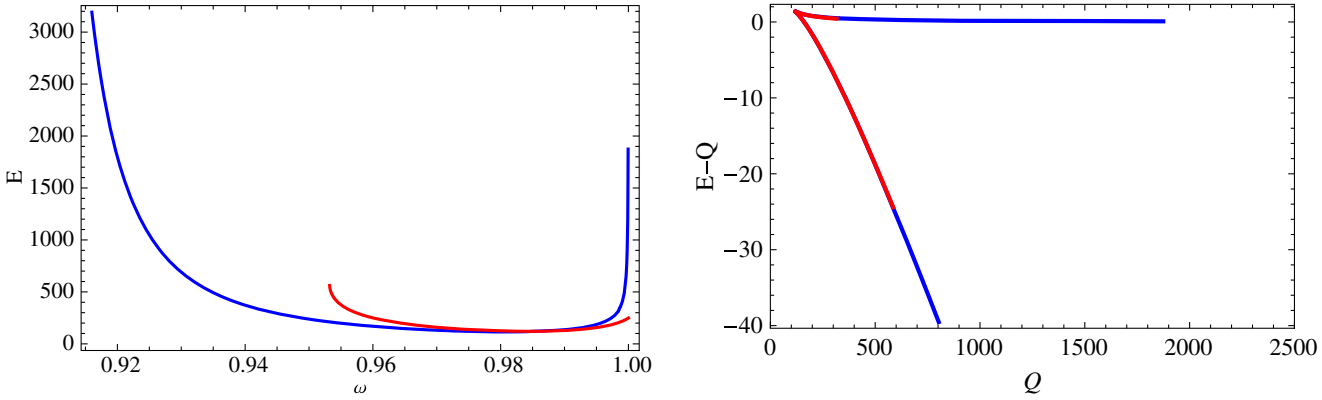

FIG. 3. (Left panel) Energy as a function of the frequency for uncharged solutions with $q = 0$ (blue curve) and charged solutions with $q = 0.02$ (red curve). The total charge follows closely the energy curve. (Right panel) Difference between the energies corresponding to the soliton and the free-boson solution as a function of the total charge (for $m = 1$). While both solitons are unstable to the decay of the free bosons in the thick-wall regime, they remain stable to this decay in the opposite thin-wall regime.

thick-wall regime (when $\omega \to 1$). We found $\omega_{\min} \approx 0.915$ for $q = 0$ and $\omega_{\min} \approx 0.953$ for $q = 0.02$.

As the soliton solutions could still decay into free bosons, it follows that an important magnitude to be analyzed is the energy difference between these two solutions, i.e., $E - mQ$. The Q dependence of this magnitude is shown in the right panel of Fig. 3. The curve obtained for $E - mQ$ consists of two branches, developing a spike at the junction point where the energy and the Noether charge of the soliton attain their minimum values. This happens at $\omega \approx 0.980$ for $q = 0$ and $\omega \approx 0.985$ for $q = 0.02$. Roughly speaking, the plot shows that both charged and uncharged solitons are unstable to the decay in the free bosons in the thick-wall regime, while stable to this decay in the thin-wall regime.

IV. PROCA STARS

In this section, we focus on the study of spherically symmetric static stars. We analyze four different types of stars—depending on the choice of the values of the Lagrangian parameters—which we name as follows:

(i) Proca stars (PS): this model was introduced in [32] and corresponds to $q = 0, m^2 \neq 0, \lambda = 0, h = 0$. For the numerics, we fix $m^2 = 1$.

(ii) Charged Proca stars (CPS): for these, we gauge the $U(1)$ symmetry of the Proca stars by setting $q \neq 0$. This is equivalent to the gauged scalar case studied in [18] with respect to the nongauged works [1,2]. Just as in the scalar case, the maximum charge is $q^2 = \frac{1}{2}$. For the numerics, we take $q = 0.5$, $m^2 = 1$, $\lambda = 0$, $h = 0$.

(iii) Self-interacting Proca stars (IPS): these solutions are gravitating solutions of Proca balls, introduced in [31] and reviewed in Sec. III, when setting $q = 0$. We will also call them Proca Q-stars since they are the Proca version of Q-stars [24]. In this case, for the numerics, we consider $m^2 = -\lambda = h = 1$.

(iv) Charged self-interacting Proca stars or charged Proca Q-stars (CIPS): the gauged version of the solutions described in the previous item. Their scalar version was studied in [25]. Again, for the numerics, we assume $m^2 = -\lambda = h = 1$, $q = \frac{1}{2}$.

For the gravitationally bounded solution, we start by assuming an ansatz for the metric

$$ds^2 = -\sigma^2(r)N(r)dt^2 + \frac{1}{N(r)}dr^2 + r^2 d\Omega_2^2. \quad (17)$$

As in the balls case studied in the previous section, we consider the ansatz (10) for the matter fields and the expression (9) for the potential.

In this case, the derived equations of motion read

$$\frac{d}{dr}\left(\frac{(u' - (\omega + qA_t)r^2)}{\sigma}\right) - \frac{r^2 u}{N^3\sigma^5}(-hu^4 + (g + 2hNv^2)Nu^2\sigma^2 - (m^2 + (g + hNv^2)Nv^2)N^2\sigma^4) = 0,$$

$$(\omega + qA_t)u' + (m^2 + (g + hNv^2)N\sigma^2v^2)N\sigma^2 v - (\omega + qA_0)^2 v - \frac{1}{N\sigma^2}(-hu^4 v + (g + 2hNv^2)\sigma^2 Nu^2 v) = 0,$$

$$A_t'' + \left(\frac{2}{r} - \frac{\sigma'}{\sigma}\right)A_t' + 2qvu' - 2q(\omega + qA_t)v^2 = 0,$$

$$N' + \frac{1}{2} grN^2 v^4 + \frac{1}{3} hrN^2 v^6 + \frac{rA_t'^2}{2\sigma^2} + \frac{ru'^2}{\sigma^2} + \frac{rv}{\sigma^2}(((\omega + qA_t)^2 + m^2 N\sigma^2)v - 2(\omega + qA_t)u')$$
$$+ \frac{ru^2}{6N^3\sigma^6}(10hu^4 - 9(g + 2hNv^2)Nu^2\sigma^2) + \frac{ru^2}{N\sigma^2}(m^2 + (g + hNv^2)Nv^2) = 0,$$
$$\frac{\sigma'}{\sigma} + \frac{r}{2N\sigma^2}\left(\frac{1}{2}A_t'^2 + \frac{\sigma^2 N'}{r}\right) + \frac{N-1}{2rN} + \frac{r}{2N\sigma^2}(u' - (\omega + qA_t))^2 + \frac{1}{2}m^2 r\left(-v^2 - \frac{u^2}{N^2\sigma^2}\right)$$
$$+ \frac{gr}{4N^3\sigma^4}(u^4 + 2N^2u^2v^2\sigma^2 - 3N^4v^4\sigma^4) - \frac{rh}{6N^4\sigma^6}(u^2 - N^2v^2\sigma^2)^2(u^2 + 5N^2v^2\sigma^2) = 0. \quad (18)$$

Near the origin, the solutions must behave as

$$u \approx u_c - \frac{u_c}{6\sigma_c}(-hu_c^4 + \sigma_c(-m^2\sigma_c^2 + \lambda u_c^2 + (\omega + qA_{tc})^2))r^2 + O(r^4),$$
$$v \approx -\frac{u_c}{3\sigma_c^2}(\omega + qA_{tc})^2 r + O(r^3),$$
$$\sigma \approx \sigma_c + \frac{1}{2\sigma_c^5}(m^2\sigma_c^4u_c^2 - \sigma_c^2\lambda u_c^4 + hu_c^6)r^2 + O(r^4),$$
$$N \approx 1 - \frac{1}{18\sigma_c^6}(6m^2\sigma_c^4u_c^2 - 9\sigma_c^2\lambda u_c^4 + 10hu_c^6)r^2 + O(r^4),$$
$$A_t \approx A_{tc} + \frac{qu_c^2}{90\sigma^6}(m^2\sigma_c^4 - \lambda\sigma_c^2u_c^2 + hu_c^4)(\omega + qA_{tc})r^4 + O(r^6). \quad (19)$$

Here, we have three free parameters, u_c, σ_c, A_{tc}, which we shall use to shoot into the proper behaviors at infinity: that is, regularity for the matter fields u, v and the gauge field A_t, and asymptotic flatness $\sigma(r \to \infty) \to 1$.

A. Results

Considering the values of m, q, λ, and h described above for the numerics, we found different sets of stars. In Fig. 4, we show the field profiles obtained for two typical cases: an interacting Proca star with $\omega = 0.876$ and a charged Proca star with $\omega = 0.926$. Later, in Fig. 5, we plot ρ and ϵ profiles for the same cases.

In the left panel of Fig. 6, we plot the Arnowitt-Deser-Misner (ADM) masses M and Noether charges Q obtained for a whole set of uncharged ($q = 0$) and charged ($q = 0.5$) Proca stars considering field frequencies in the $\omega \sim 0.80$–1.0 range. For all cases, as $\omega \to 1$, both M and Q of the solutions vanish, while $Q/M \to 1$. In this limit, Proca stars become large and light, with very low mean densities, with trivial results at $\omega = 1$. On the other hand, for smaller ω's, Proca stars get more compact. Both in the uncharged and charged cases, M and Q follow a spiral, towards different central configurations depending on the choice of q. For $q = 0$, this critical configuration is located around $\omega \approx 0.89$ [32], while, for $q > 0$, this critical value becomes larger. Moreover, while for $q = 0$ the maximum of both M and Q occurs at $\omega_{\max} \approx 0.875$, with $M_{\max} < Q_{\max} \approx 1$, all of the critical values increase for $q > 0$. Regarding the stability of these solutions, in the lower part of the spirals, $M > Q$, and thus the binding energy $E = 1 - M/Q$ becomes negative, making all of these regions unstable against perturbations [32]. An analogue behavior is found for the self-interacting cases, which follow similar trends in all cases, as can be seen in the right panel of Fig. 6.

Finally, in the left panel of Fig. 7, we show the total ADM mass M as a function of the central density $u(0)$ for the four cases considered in this section: (un)charged Proca

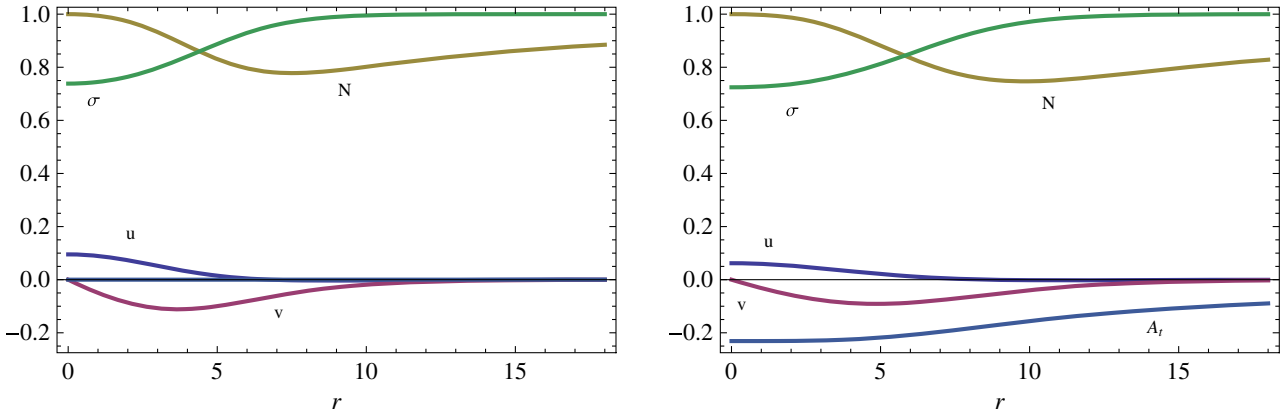

FIG. 4. (Left panel) Profiles of an interacting Proca star with $\omega = 0.876$. (Right panel) Profiles of a charged interacting Proca star of $\omega = 0.926$.

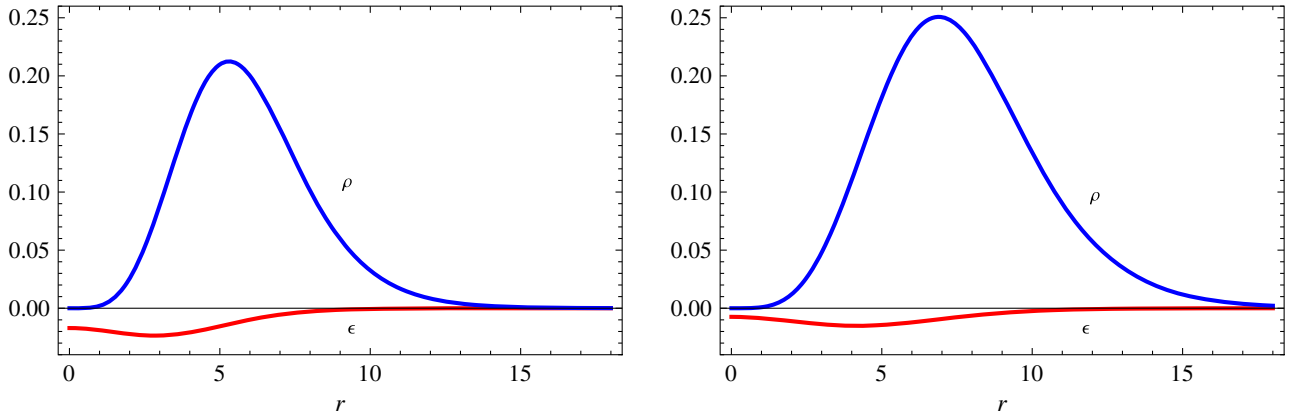

FIG. 5. Charge and energy-density profiles of (left panel) the interacting Proca star of $\omega = 0.876$ and (right panel) the charged interacting Proca star of $\omega = 0.926$.

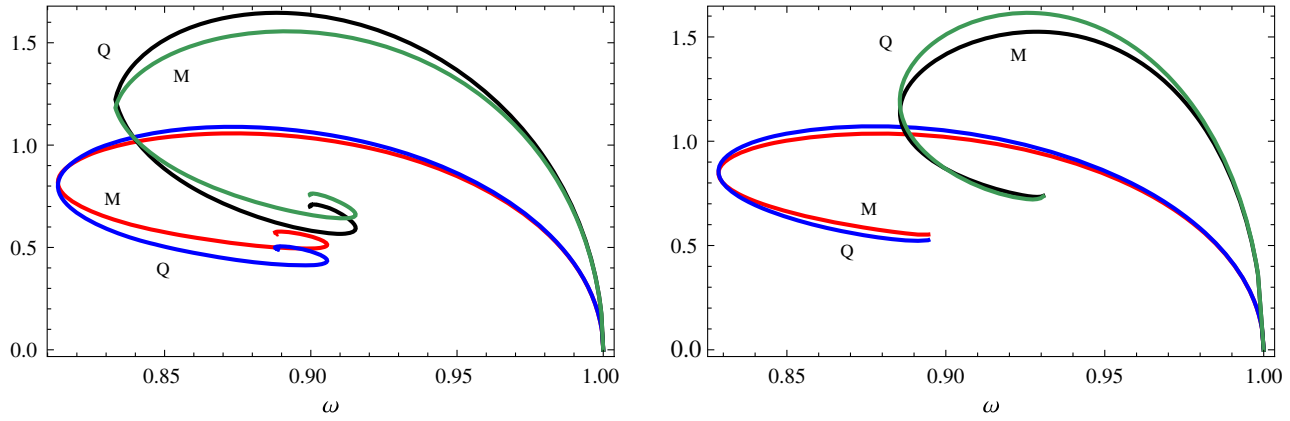

FIG. 6. (Left panel) ADM mass M and Noether charge Q for the Proca star (red and blue, respectively) and the charged Proca star (green and black, respectively) with respect to the Proca field frequency ω. (Right panel) The same magnitudes for the self-interacting case.

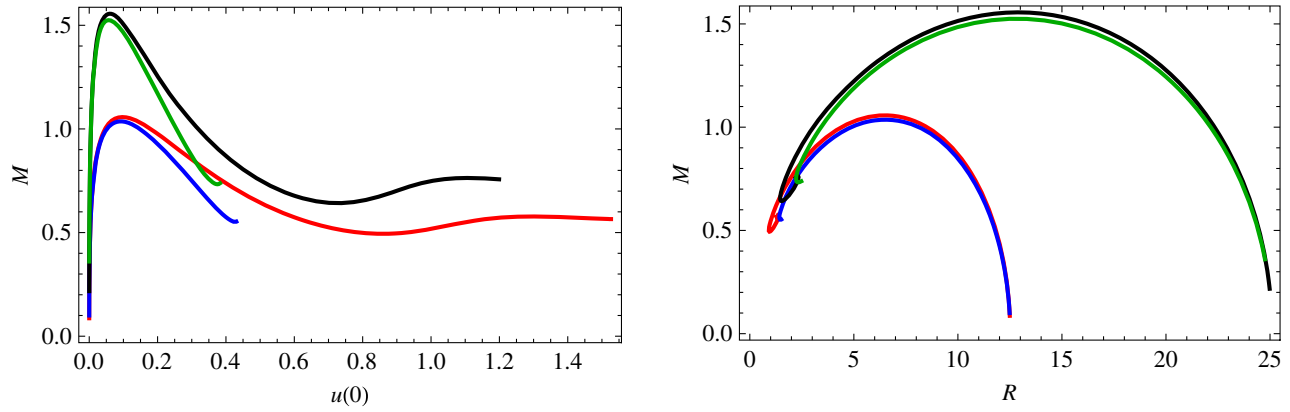

FIG. 7. ADM mass M as a function of (left panel) the central density $u(0)$ and (right panel) the radius R for the Proca star (red), the charged Proca star (black), the self-interacting Proca star (blue), and the charged self-interacting Proca star (green).

TABLE I. Maximum masses and minimum radii for the different solutions expressed first in dimensionless units (for $m = 1$) and then in physical units of solar masses ($M_\odot$) and kilometers (km) for $m = 10^{-10}$ eV.

	PS		IPS		CPS		CIPS	
m	$M_{\max}$	$R_{\min}$	$M_{\max}$	$R_{\min}$	$M_{\max}$	$R_{\min}$	$M_{\max}$	$R_{\min}$
$m = 1$	1.05	6.92	1.04	6.50	1.56	12.88	1.52	12.96
10^{-10} eV	1.40 $M_\odot$	13.69 km	1.39 $M_\odot$	12.86 km	2.09 $M_\odot$	25.48 km	2.03 $M_\odot$	25.64 km

stars and (un)charged self-interacting Proca stars. In the right panel of Fig. 7, we plot the mass-radius profiles of the same solutions. In order to do so, we define the radius of the Proca Star as [18]

$$R = \int d^3x\sqrt{-g}rj^0. \tag{20}$$

While uncharged and charged versions of both Proca and self-interacting stars show very similar trends in the mass-radius diagrams for the same parameters, they show a very different dependence on the central density, as the left panel of Fig. 7 evidences. In both families, the gauged-star versions are more massive and less compact than the uncharged ones.

We worked in natural units but also while setting $m = 1$. In order to recover physcal units, a physical value for the particle mass must be assumed. In Table I, we show maximum masses and minimum radii for a canonical case. Note that both the mass and the radius are measured in units of M_{pl}^2/m, where M_{pl} is the Planck mass. Then the compactness $\eta = \frac{2M}{R}$ is independent of the particle mass (for each of the families considered). For our solutions, we find $\eta_{\max} = 0.30$ (PS), 0.32 (IPS), 0.24 (CPS), and 0.23 (CIPS), which are, of course, less than the Schwarzschild black-hole value $\eta = 1$.

V. CONCLUSIONS

We studied a broad class of spherically symmetric regular solutions involving a complex massive vector.

First, we studied Proca Q-balls, that is, nongravitating solutions with a self-interaction potential which acts to hold the system together. We found both charged and uncharged solutions of this particular class of Q-balls below a critical charge, depending on the choice of the free parameters available. For both charged and uncharged cases, we found that solutions are only allowed in a limited range of frequencies $\omega_{\min} < \omega < m$, with divergent energy in both minimum and maximum frequencies. This extrema defined the so-called thin-wall ($\omega \to \omega_{\min}$) and thick-wall ($\omega \to m$) regimes. Moreover, analyzing in detail the $E - mQ$ relation, we concluded that, in the thick-wall regime, the solutions are unstable and will decay into free "procons" or free Proca states.

Second, we also studied Proca stars and Proca Q-stars, that is, self-gravitating solutions. At that point, we extended the results of [32] for a broader class of potentials showing that the self-gravitating solutions were indeed robust. In this sense, since it is reasonable to assume that dark matter in the Universe could be composed of different kinds of fundamental entities, condensates as vector Proca stars studied here, as scalar boson stars analyzed elsewhere represent another viable dark component.

Looking forward, the next steps in this study could come from extending our spherically symmetric solutions to allow for rotation in order to investigate spinning Proca Q-balls, which could be done by considering a vector version of spinning nontopological solitons made of scalar fields [38–42]. In the same direction, it would also be interesting to find solutions where these fields act like a Kerr black-hole hair or clouds following the steps of [9–13,15]. On the other hand, clouds may also exist surrounding static black holes [14]. Extending the solutions found in this paper for our self-interacting model would then be a promising future approach to this field as well.

ACKNOWLEDGMENTS

We are grateful to the referee for his/her insightful comments. I. S. L. and F. G. acknowledge support from CONICET, Argentina. We would like to thank Raulo Arias for carefully reading this manuscript. I. S. L. would like to thank Juli for the hospitality and amenities during several stages of this project. I. S. L. thanks the IFLP, ICTP, and Galileo Galilei Institute for Theoretical Physics for their hospitality. F. G. is grateful to Luz and Paz for the cordial reception.

[1] D. J. Kaup, Klein-Gordon geon, Phys. Rev. **172**, 1331 (1968).
[2] R. Ruffini and S. Bonazzola, Systems of self-gravitating particles in general relativity and the concept of an equation of state, Phys. Rev. **187**, 1767 (1969).
[3] F. E. Schunck and E. W. Mielke, General relativistic boson stars, Classical Quantum Gravity **20**, R301 (2003).
[4] S. L. Liebling and C. Palenzuela, Dynamical boson stars, Living Rev. Relativ. **15**, 6 (2012).

[5] Z. Meliani, F. H. Vincent, P. Grandclément, E. Gourgoulhon, R. Monceau-Baroux, and O. Straub, Circular geodesics and thick tori around rotating boson stars, Classical Quantum Gravity **32**, 235022 (2015).
[6] P. Grandclement, C. Somé, and E. Gourgoulhon, Models of rotating boson stars and geodesics around them: New type of orbits, Phys. Rev. D **90**, 024068 (2014).
[7] F. H. Vincent, Z. Meliani, P. Grandclement, E. Gourgoulhon, and O. Straub, Imaging a boson star at the Galactic center, Classical Quantum Gravity **33**, 105015 (2016).
[8] P. V. P. Cunha, C. A. R. Herdeiro, E. Radu, and H. F. Runarsson, Shadows of Kerr black holes with and without scalar hair, Int. J. Mod. Phys. D **25**, 1641021 (2016).
[9] S. Hod, Stationary scalar clouds around rotating black holes, Phys. Rev. D **86**, 104026 (2012); **86**, 129902(E) (2012).
[10] S. Hod, Kerr-Newman black holes with stationary charged scalar clouds, Phys. Rev. D **90**, 024051 (2014).
[11] C. L. Benone, L. C. B. Crispino, C. Herdeiro, and E. Radu, Kerr-Newman scalar clouds, Phys. Rev. D **90**, 104024 (2014).
[12] C. Herdeiro, E. Radu, and H. Runarsson, Non-linear Q-clouds around Kerr black holes, Phys. Lett. B **739**, 302 (2014).
[13] C. A. R. Herdeiro and E. Radu, Kerr Black Holes with Scalar Hair, Phys. Rev. Lett. **112**, 221101 (2014).
[14] M. O. P. Sampaio, C. Herdeiro, and M. Wang, Marginal scalar and Proca clouds around Reissner-Nordström black holes, Phys. Rev. D **90**, 064004 (2014).
[15] C. Herdeiro, E. Radu, and H. Runarsson, Kerr black holes with Proca hair, Classical Quantum Gravity **33**, 154001 (2016).
[16] H. Dehnen and B. Rose, Flat rotation curves of spiral galaxies and the dark matter particles, Astrophys. Space Sci. **207**, 133 (1993).
[17] D. F. Torres, Boson stars in general scalar-tensor gravitation: Equilibrium configurations, Phys. Rev. D **56**, 3478 (1997).
[18] P. Jetzer and J. J. van der Bij, Charged boson stars, Phys. Lett. B **227**, 341 (1989).
[19] S. R. Coleman, Q balls, Nucl. Phys. **B262**, 263 (1985); **B269**, 744(E) (1986).
[20] I. E. Gulamov, E. Y. Nugaev, and M. N. Smolyakov, Theory of $U(1)$ gauged Q-balls revisited, Phys. Rev. D **89**, 085006 (2014).
[21] F. Paccetti Correia and M. G. Schmidt, Q balls: Some analytical results, Eur. Phys. J. C **21**, 181 (2001).
[22] I. E. Gulamov, E. Y. Nugaev, A. G. Panin, and M. N. Smolyakov, Some properties of $U(1)$ gauged Q-balls, Phys. Rev. D **92**, 045011 (2015).
[23] K. M. Lee, J. A. Stein-Schabes, R. Watkins, and L. M. Widrow, Gauged Q balls, Phys. Rev. D **39**, 1665 (1989).
[24] B. W. Lynn, Q-stars, Nucl. Phys. **B321**, 465 (1989).
[25] A. Prikas, Q-stars and charged q-stars, Phys. Rev. D **66**, 025023 (2002).
[26] M. Colpi, S. L. Shapiro, and I. Wasserman, Boson Stars: Gravitational Equilibria of Selfinteracting Scalar Fields, Phys. Rev. Lett. **57**, 2485 (1986).
[27] B. Hartmann, B. Kleihaus, J. Kunz, and I. Schaffer, Compact boson stars, Phys. Lett. B **714**, 120 (2012).
[28] S. Kumar, U. Kulshreshtha, and D. S. Kulshreshtha, New results on charged compact boson stars, Phys. Rev. D **93**, 101501 (2016).
[29] S. Kumar, U. Kulshreshtha, and D. S. Kulshreshtha, Boson stars in a theory of complex scalar field coupled to gravity, Gen. Relativ. Gravit. **47**, 76 (2015).
[30] F. E. Schunck and D. F. Torres, Boson stars with generic self-interactions, Int. J. Mod. Phys. D **9**, 601 (2000).
[31] A. Y. Loginov, Nontopological solitons in the model of the self-interacting complex vector field, Phys. Rev. D **91**, 105028 (2015).
[32] R. Brito, V. Cardoso, C. A. R. Herdeiro, and E. Radu, Proca stars: Gravitating Bose-Einstein condensates of massive spin 1 particles, Phys. Lett. B **752**, 291 (2016).
[33] R. Brito, V. Cardoso, and H. Okawa, Accretion of Dark Matter by Stars, Phys. Rev. Lett. **115**, 111301 (2015).
[34] R. Brito, V. Cardoso, C. F. B. Macedo, H. Okawa, and C. Palenzuela, Interaction between bosonic dark matter and stars, Phys. Rev. D **93**, 044045 (2016).
[35] E. Seidel and W. M. Suen, Oscillating Soliton Stars, Phys. Rev. Lett. **66**, 1659 (1991).
[36] R. G. Cai, L. Li, and L. F. Li, A holographic p-wave superconductor model, J. High Energy Phys. 01 (2014) 032.
[37] R. G. Cai, S. He, L. Li, and L. F. Li, A holographic study on vector condensate induced by a magnetic field, J. High Energy Phys. 12 (2013) 036.
[38] M. S. Volkov and E. Wohnert, Spinning Q-balls, Phys. Rev. D **66**, 085003 (2002).
[39] V. Benci and D. Fortunato, Spinning Q-balls for the Klein-Gordon-Maxwell equations, Commun. Math. Phys. **295**, 639 (2010).
[40] Y. Brihaye, Th. Caebergs, and T. Delsate, Charged-spinning-gravitating Q-balls, arXiv:0907.0913.
[41] B. Kleihaus, J. Kunz, and M. List, Rotating boson stars and Q-balls, Phys. Rev. D **72**, 064002 (2005).
[42] F. D. Ryan, Spinning boson stars with large self-interaction, Phys. Rev. D **55**, 6081 (1997).